Numerical Analysis of the Effect of Different Entrance Lengths of the Flanged Shroud on the Power Performance of Savonius Rotor

Alsaied Khalil*, M.M Bassuoni*, M.F.Obiaa*‡, Ahmed M.Khaira*

*Department of Mechanical Power, Faculty of Engineering, Tanta University, Tanta- Egypt P.O. 31733

(akhalil@f-eng.tanta.edu.eg, m.mahgoub@f-eng.tanta.edu.eg, mohamed_obiaa@f-eng.tanta.edu.eg, ahmed.khaira@f-eng.tanta.edu.eg)

‡Corresponding Author; Third Author, P.O. 31733(Tanta-Egypt), Tel: +201282454050, Fax: +20403453860, mohamed_obiaa@f-eng.tanta.edu.eg

Received: 07.12.2023 Accepted:29.01.2024

Abstract- In this study, the effect of the different entrance lengths (short, medium, and long) of the flanged shrouded Savonius rotor is investigated in three-dimension (3-D) numerically by ANSYS-FLUENT 2022 R1. The current numerical model of a simple rotor, which has an equal diameter and height of 300 mm, is validated with the previously published experimental results of the same rotor at the same operating condition (wind speed 6 m/s) and geometry. The validation is done by the several turbulence models which are recommended by the previous published numerical studies with different values of time step size and mesh size. The numerical and experimental power curves indicate good agreement with each other when using the SST K-ω model with a time step size of 0.0025 s with an accuracy percentage around 96 %. The analysis of the numerical results of the three flanged shrouded models shows an enhancement of the torque coefficient at tip speed ratio 0.42 with a 40% increase and the power coefficient at tip speed ratio 0.5 with an 18% increase compared with the bare rotor at the same free stream velocity. However, the shroud is not effective on the performance of the rotor after a tip speed ratio of 0.7.

Keywords Savonius; CFD; Shroud; Wind; VAWT.

Nomenclature

C_p	Power coefficient (dimensionless)
C_t	Torque coefficient (dimensionless)
T	Torque (N.m)
Ω	Angular speed of rotor (rad/s)
ρ	Air density (kg/m^3)
U	Wind velocity (m/s)
H	Rotor height (m)
D	Rotor diameter (m)
D_m	Model diameter (m)
D_o	Endplate diameter (m)
R	Rotor blade radius (m)
λ	Tip speed ration (ω.r)/(U) (dimensionless)
A_s	Aspect ratio (H/D)
a	Overlap distance (m)
G	Overlap ratio (a/2r) (dimensionless)

1. Introduction

Today, governments and individuals have a big financial issue in the energy sector. All of them suffer from a continuous price rising of fossil fuel. Also, no one can neglect the side effect of the huge emissions from fossil fuel combustion which causes several environmental issues like acid rain and global warming. These problems led the world to depend more on green and sustainable energy resources like wind, solar, tidal, and hydro[1-3].

According to the Global Wind Energy Council (GWEC) report in 2023 [4], the increase in the world wind capacity installations three years ago is the biggest in history. Around 88.8 GW of wind capacity is installed annually globally, and the experts expect that 680 GW of new wind capacity will be installed globally over the next five years. That is because the wind is one of the cheapest renewable energy resources in the world. Besides, its availability in whole areas encourages many researchers to continuously focus their research [5-6].

The Savonius turbine is one of the most famous wind turbine types and belongs to the vertical-axis wind turbine category. It has been constructed based on a very simple concept from oil drums, and it has been used successfully [7]. This type of turbine is highly desired in underdeveloped countries due to its simple construction, ease of operation, and low maintenance. Hence, the low capital cost of this machine, which mainly determines power costs, supports using it, although its efficiency is not high.

2. Literature review

It is well known that the power coefficient of Savonius wind turbine is very low compared to other types in its category. However, researchers did more trials to enhance and develop its performance to gain more power especially at low wind speed.

The researchers in this field are trying day by day to raise up the performance of Savonuis rotor type to be more beneficial in the market. This development is taking two directions. The first one is by the enhancement of the blade rotor such as geometry, gap, overlap, number of rotors, end plate, etc. The other direction is by optimizing the augmented objects such as obstacle, deflector, guide box, guide vanes, etc. In this work, we are following the second direction for enhancing the Savonius performance. First, relevant work is reviewed and then the aim of this research is presented.

This literature review presents the contributions of researchers in the second direction of Savonius performance enhancement.

This part presents the influence of obstacles, curtains and deflectors on the rotor performance in the different studies. Abdelmordy et al. (2022) [8], examined numerically and experimentally the influence of obstacles with different positions on the performance of shrouded Savonius rotor. Their results indicated the numerical results were very close to the experimental results which showed the increasing of power coefficient by 31% compared with the bare one. T.Ogawa and H.Yoshida (1986) [9] examined the effect of three types of deflecting plates on the performance of traditional Savonius's rotor in a test section of wind tunnel which had air speed of around 7 m/s. Their results indicated that the most effective deflector plate is simple one which resulted in 24% increase of power coefficient. B. Altan et al. (2008) [10] carried out experiments on Savonius wind turbines with curtains at different angles and dimensions by using open wind tunnel where the air speed was 7m/s. The experimental results had reached the optimum geometric of curtain that had decreased the negative torque and maximized the inlet free stream velocity which increased the power coefficient to 0.38. Youssef et al. (2019) [11] tested the impact of using upstream and downstream plate deflector on the output of traditional Savonius type. The numerical analysis indicated to raise up of the power coefficient reached 0.47 at tip speed ratio 1. Zhang et al. (2020) [12] had introduced a novel arc shape of rotor. The curtain angles were tested both numerically and experimentally to get the optimum angles. The maximum "C_p" reached 0.3 occurred at an optimum angle 15°. Yuwono et al. (2020) [13] replaced the plate deflector with a small cylinder with a diameter equals to 0.5 of the Savonius cylinder rotor diameter. The experimental results presented the enhancement of power coefficient where the small cylinder located 1.4 times the cylinder diameter far of rotor. The maximum "C_p" reached 0.2 at "λ" 0.65 that mean 12% increase compared with the conventional one. Mohamed et al. (2021) [14] used the optimization algorithm coupled with CFD to obtain the optimum positions and geometry of the deflectors. Their results indicated that the optimum configuration had a power coefficient's increase by 35.5% at tip speed ratio 0.9. Mohamed et al. (2011) [15] obtained the optimized of the shape of Savonius blade which was augmented with plate obstacle by using optimizer and CFD code coupling. The k-Ɛ turbulence model was the more accurate model which and validated with the previous experimental result. The optimum blade with obstacle plate reached the highest "C_p" 0.389 at tip speed ratio "λ" 0.7. Kaprawi et al. (2015) [16] studied experimentally the performance of combined Darrius and Savonius turbines with and without deflector with different angles. Their results showed enhancement of power coefficient and torque coefficients reached by 18% and 16%, respectively, compared with solo Darrius turbine. Shouman et al. (2022) [17] investigated numerically by ANSYS FLUENT 16 the effect of optimized arrangement of curtain with adding fins on the blade. The maximum "C_p" of the Savonius rotor was increased by about 42% with the optimum curtain arrangement. Tian et al. (2022) [18] improved the performance of Savonius rotor using passive deflector which could move with reference to direction of wind by connected tail. Their numerical results showed a remarkable enhancement of performance. The capability of the rotor's output was increased by 24.91% by using the passive deflector.

Here, the effect of different types of guide vanes is shown through the following studies. In 2022, W. Senarathna et al. [19] enhanced the output of Savonius rotor by using optimized configurated blades which augmented with omnidirectional guide vanes. Their numerical analysis indicated an increase of the power coefficient with 80% obtained at tip speed ratio 0.8. Z. Mu et al. (2022) [20] studied the performance of modified blade under different conditions. They found the turbine starting can be done at any angle compared with the conventional that can not start the rotation from 120 to 170°. Also, the stability and efficiency of the modified blade resulted in torque coefficient increase by 36%. P. Apparavoo et al. (2022) [21] numerically studied, in two-dimensional (2-D) analysis, the effect of guide vanes and shield with different angles on the performance of rotor located in a solar chimney. They observed higher power coefficient reached to 0.44, occurred at angle 45°, with an increase of power by around 22% compared with turbine without vanes and shield. Yahya et al. (2021)[22] studied experimentally by wind tunnel the impact of the different values of tilt angle and the different number of guide vane blades on the output of Savonius rotor. They found that the maximum power performance occurred at six blades of guide vanes and with tilt angle equals 60° at different wind speed. Siregar et al. (2021) [23] recorded the pressure distribution of Savonius blade with several numbers of omnidirectional guide vane model. The power coefficient increased, when using 12 guide vanes, by 25% at tip speed ratio 0.9. Also, it was observed that the static torque decreased when the guide blades were increased to 16 blades.

The main function of turbine's casing is concentrating and accelerating the wind towards turbine's rotor. In this part the effect of casing is presented by several trials. Elbatran et al. (2017) [24] performed a numerical investigation using ANSYS ICEM to examine the performance of ducted nozzle water Savonius wind turbines. Their results showed that the maximum power coefficient reached 0.27 at tip speed ratio 0.73 which means increasing of power generated by 78%

compared with the convectional one. k. Irabu and J.Roy (2007) [25] used a guide box tunnel to enhance the conventional Savonius power performance. Their experiments had been performed for two- and three-blades models in the wind tunnel test section. Their results indicated that the power coefficient C_p was raised by one and half times for the three blades and one and fourth times for the two blades compared with bare one. Mohammadi et al. (2018) [26] proposed a new technique to maximize the power performance by testing numerically four different nozzle models placed in the front of the facing concave blade. Their results showed an enhancement of the performance where the "C_p" increased from 0.16 to 0.39. E. Anter and M. Elkhoury (2019) [27] numerically tested several models of casing Savonius turbine and they found that two dimension (2-D) based simulation was not accurate compared with three dimensional (3-D) based one. The 3-D-based simulation results had been validated and indicated to a power coefficient enhancement of cased turbine that reached 0.425 at tip speed ratio 0.59.

From the aforementioned survey, it is noted that some researchers enhanced the Savonius output by adding fixed objects such as a curtain, plate obstacle, and guide box in front of the returning blade to reduce the negative drag force. Although the output power was increased, these different ideas made the Savonius unable to work in any wind direction. Other researchers developed the rotor augmented with guide vanes. The increase in torque and power performance was obtained, and the rotor can be operated from any wind direction. But their models' constructions were not simple and cheap, which are the most popular advantages of Savonius.

In this study, the effect of the different entrance lengths of flanged diffuser shroud on the simple Savonius rotor is studied 3-D numerically by ANSYS-FLUENT 2022 R1. The shroud is very simple in design, easy to fabricate, and self-rotated according to the wind direction under the influence of drag force. Here, it was focused on the effect of the shroud entrance's length on the rotor performance by analyzing the power and torque coefficients against the tip speed ratio and comparing them with the conventional turbine's results under the same conditions.

3. Physical model

3.1. Savonius Rotor Model

The Savonuis rotor used in this study has the same geometry and material specification which Fujisawa and Gotoh used [28, 29], as shown in “Figure 1".

This model has a height (H) of 300 mm and a rotor diameter (D) of 300 mm that lead to an aspect ratio (As) equals one. The thickness of the blade (t) is 2 mm, and this rotor is augmented with end plates up and down of a diameter (D_o) 330 mm. The overlap ratio (G) is 0.15 and gap ratio equals zero where the power coefficient reached the optimum, where (a) and (R) represent the overlap distance and rotor radius, respectively.

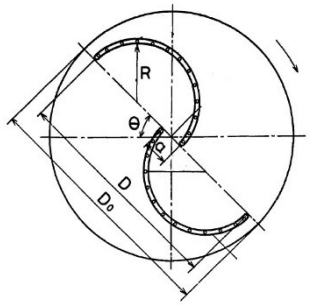


Fig. 1. Simple semicircular savonius rotor, rotor height (H), rotor diameter (D), blade thickness (t), end plate diameter (D_0), overlap ratio (a), gap ratio (G) [28].

$$\text{Aspect ratio } (A_s) = H/D \quad (1)$$

$$\text{Overlap ratio } (G) = a / (2*r) \quad (2)$$

3.2. Flanged Shrouded Models

It is well known that the potential power generated from any wind turbine is proportional to the cubic value of wind speed. So, any enhancement of wind speed reflects a large enhancement of energy output.

Shrouded and flanged shrouded wind turbines are one of the important techniques used to enhance the power coefficient of wind turbines. El-Zahaby et al. [30] developed the shape of flanged shroud for horizontal axis wind turbine and reached to a good enhancement in generated power by the rotor.

In this research, the effect of the flanged shroud with an optimum flange angle, which was early examined on the horizontal axis wind turbine by El-Zahaby et al. [30], is studied on the performance of Savonuis rotor, as shown in "Figure 2, 3", was examined numerically. It was also compared with the bare rotor at the same conditions which are: the diffuser angle θ_2= 10°, diffuser length L_2= 200mm, flange angle θ_3= 12°, L_3 =100 mm, and θ1= 5°. As shown in “Figure 2”, L_1 represents the entrance length, L_2 represents the diffuser length and L_3 represents the flange length.

The entrance length (L_1) of the flanged shroud was examined to obtain the optimal one by three different models short, medium, and long as clarified in "Table 1." and compared with bare rotor.

Table 1. Lengths of shroud's entrance of the three tested models

No.	Shroud size	Entrance length (L_1)
1	Short	100 mm
2	Medium	250 mm
3	Long	400 mm

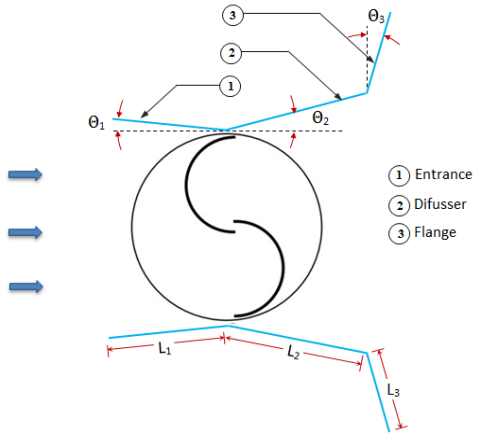


Fig. 2. Flanged shroud of Savonius rotor, entrance length (L_1), diffuser length (L_2), flange length (L_3), entrance angle (θ_1), diffuser angle (θ_2), flange angle (θ_3).

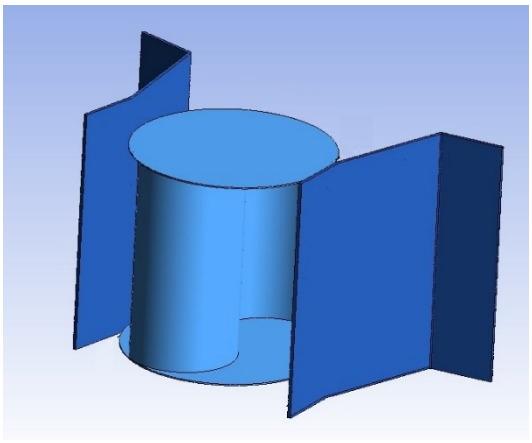


Fig. 3. Isometric view of the flanged shroud Savonius rotor.

4. Numerical method

In this work, a commercial package ‘‘ANSYS-FLUENT 2022, R1” is used to perform the three-dimensional (3-D) simulation using an HP workstation in the mechanical lap of faculty of engineering at Tanta university. The geometries of the models were designed and created by the commercial package “SOLIDWORKS” and were converted to the proper file format for the “FLUENT” reader.

4.1. Domain and Boundary Conditions

The 3-D model and its domain were designed by “SOLIDWORKS” and converted to “ANSYS FLUENT MODELER” for identifying the boundaries and operating conditions as shown in "Figure 4, 5". The computational domain is divided to two parts separated by a sliding interface: a rotating domain (circular zone) and a fixed domain which is an open tunnel with the rotating domain excluded from it. The fixed domain consists of four surrounding walls with inlet and outlet sides.

From literature survey, the minimum dimensions of domain to avoid the turbulence effect of wall turbulence on the accuracy of result is ($10D_m$ *$10\ D_m$*$15\ D_m$), where D_m is the model diameter. The rotor, located at the center of the rotating domain, is placed at a distance $5D_m$ from the top and bottom sides of the rectangular domain, and at a $5D_m$ distance upwind, where the condition of inlet velocity U = 6 m/s.

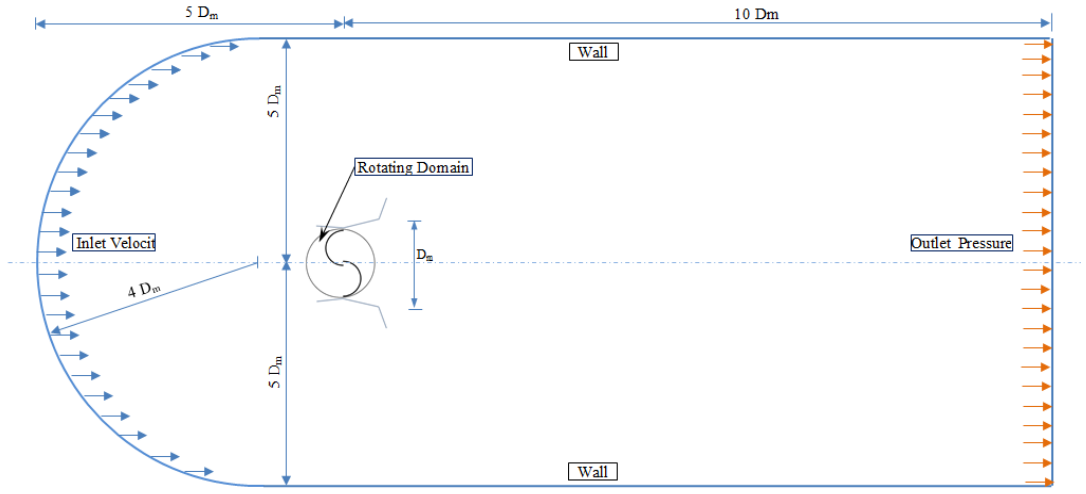


Fig. 4. Plan view of the numerical domain with boundary conditions.

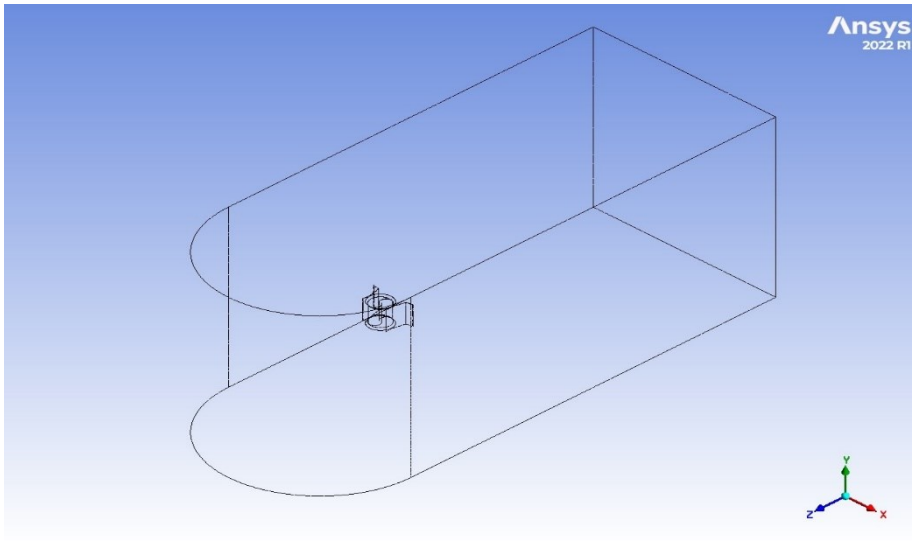


Fig. 5. Isometric view of 3-D numerical domain at ANSYS FLUENT 2022 R1.

4.2. Mesh Test

The mesh sizing is very important step of 3-D ANSYS FLUENT simulation process to get a high accuracy with avoiding the shortage of convergence. The mesh test was investigated by five trials of different element numbers starting from 1,990,879 elements (as a coarse mesh grid) to 5,916,446 elements (as a fine mesh grid), as shown in "Table 2.". The highest torque coefficient (C_t) of Savonius rotor is taken as the main parameter to determine the accuracy of the trials. Almost identical values of Ct are obtained at numbers of elements 5,916,446 and 4,956,350 (cases no. 1 & 2) in "Table 2." with an error around 0.3%, which is accepted and closed to the experimental result.

Table 2. Grid element of mesh test

No.	Number of elements	Torque coefficient Ct
1	5,916,446	0.266
2	4,956,350	0.265
3	3,560,256	0.276
4	2,347,389	0.285
5	1,990,879	0.29

The grid density is not distributed homogenously at the whole domain. The highest grid densities are located in the regions of the rotating domain and downstream where the vortices are generated as shown in "Figure 6". However, the size of mesh in the interface boundary between the rotating and fixed domains must be the same at two all interface sides. Also, the growth rate of inflation's layer around the turbine blade and shroud walls was used with a suitable rate 1.2 to account for changing the mesh size. In this study five layers of inflation is used as shown in "figure 7".

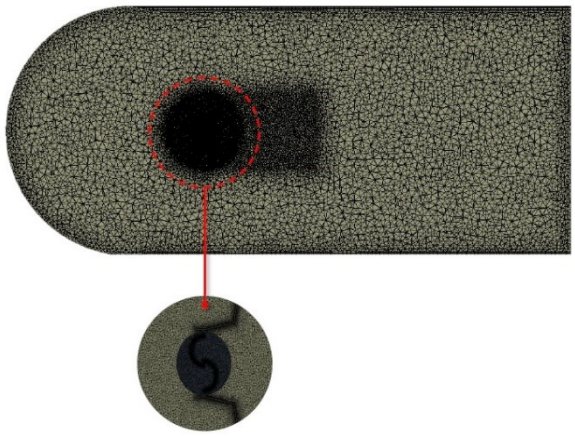


Fig. 6. Mesh of fixed and rotating domains.

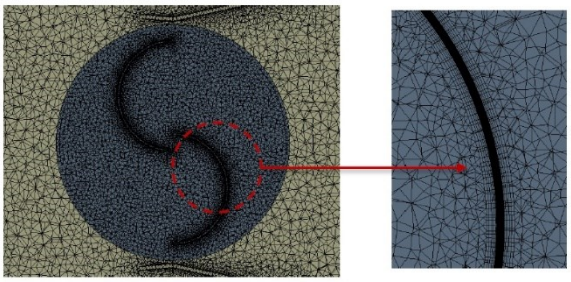


Fig. 7. Mesh inflation layers for rotor blade's wall.

4.3. Time Step Size Test

Most transient simulations consist of a considerable number of time steps. Therefore, the choice of the time step size is critical for the accuracy of transient simulations. In this study, the value of time step was decreased gradually from big to small to get the optimum one.

"Figure 8" displays the model results between rotational speed and time at several values of time step size starting from 0.075s down to 0.0012s. It is shown that the results of time

step sizes of 0.0025s and 0.00125s are identical. So, decreasing the time step more than 0.0025s yields no change in the results and the solution will take more time without any benefits. This means that the time step size 0.0025s is the optimum one.

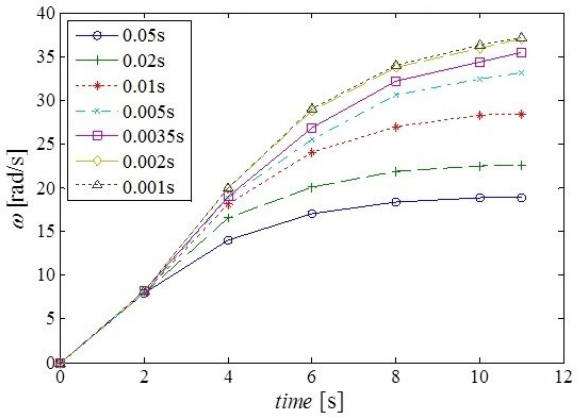


Fig. 8. Rotational speed against time of Savonius rotor at different time step size.

4.4 Model Validation

Five turbulence models; standard K-ε, RNG K-ε, Realizable K-ε, SST K-ω and SST transition were examined to find the proper model in this case. The models were investigated at the same conditions of Fuijisawa's experimental study [28] which are: velocity of free stream U = 6 m/s and diameter of rotor D and height H are both equal to 300 mm.

"Figure 9" shows the models' results between torque coefficient and tip speed ratios which were compared with the reference to the previous experimental results [28]. The results show that SST K-ω is very close to the published experimental results.

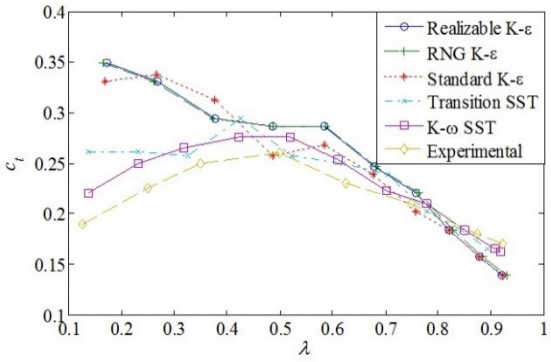


Fig. 9. Torque coefficient and tip speed ratio at different turbulence models.

5. Results and Discussion

In this study the important parameters such as torque T , rotational speed ω, torque coefficient C_t and Power coefficient C_p were analyzed for three shrouded models and compared with the un-shrouded conventional rotor for determining and obtaining the enhancement for each one. In the following, the pressure and velocity contours are shown and explained at two positions of the rotors for all models. The first position is where the rotor, with its two blades, are facing the free stream, while the other position is in parallel with the free stream.

5.1 First Position: Rotor's Blade Facing the Free Stream

The pressure contours for the four models shown in "Figures 10, 11, 12, and 13" validated the working concept of the Savonius turbine as a drag machine. The pressure reaches its highest value due to the accumulation on the concave and convex surfaces of the blade from the inlet direction which causes the rotation of rotor. Also, it is obtained that the highest pressure zone in the domain for all shrouded rotors is increased in proportion to the entrance length of the shroud.

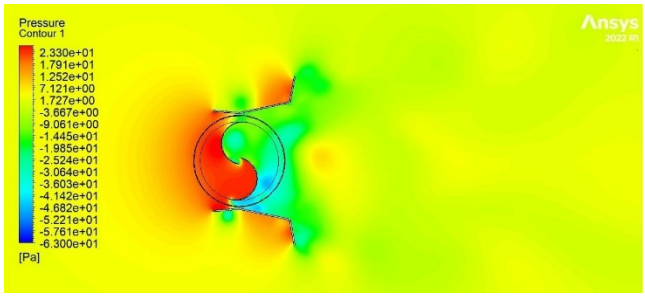


Fig. 10. Pressure contour of short flanged shrouded rotor at first position.

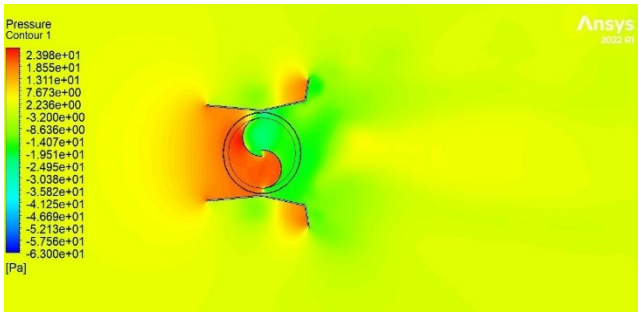


Fig. 11. Pressure contour of medium flanged shrouded rotor at first position.

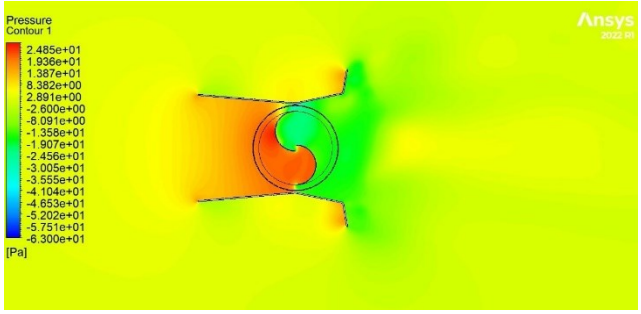


Fig. 12. Pressure contour of long flanged shrouded rotor at first position.

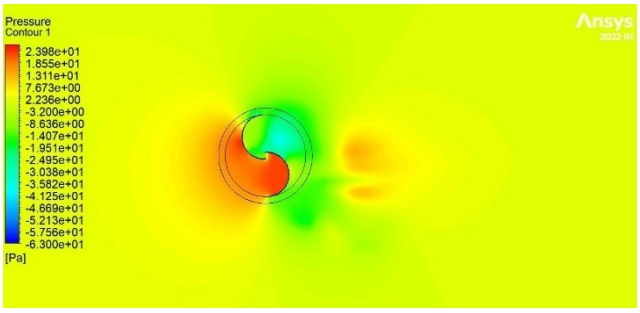


Fig. 13. Pressure contour of un- shrouded (bare) rotor at first position.

The velocity contours of the four models are shown in "figures 14, 15, 16, and 17", which indicate a stagnation zone before the concave and convex blades. But, here, it is very clear that the stagnation on the concave surface at all models is greater than on the convex surface, which is the mean reason for the drag force difference that causes the rotation.

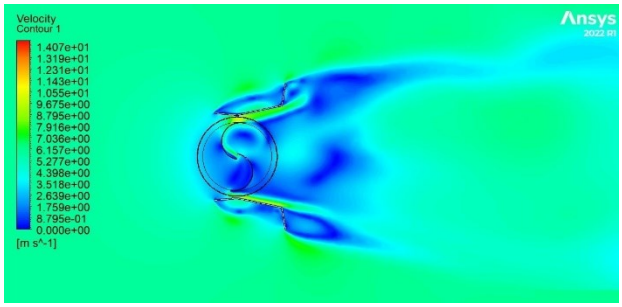


Fig. 14. Velocity contour of short flanged shrouded rotor at first position.

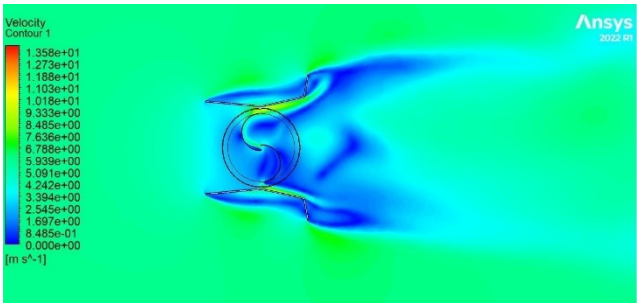


Fig. 15. Velocity contour of medium flanged shrouded rotor at first position.

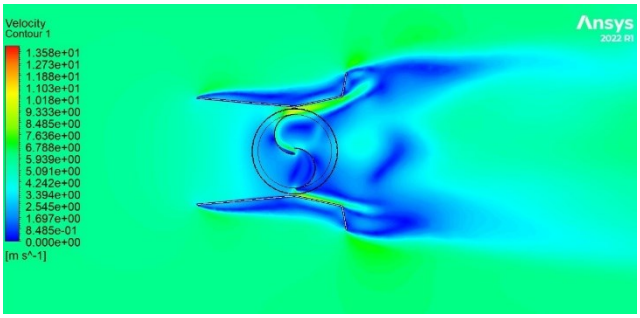


Fig. 16. Velocity contour of long flanged shrouded rotor at first position.

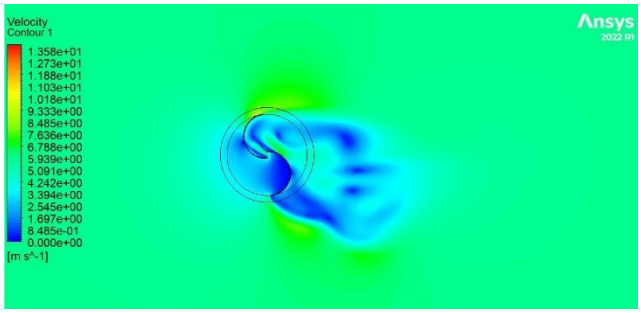


Fig. 17. Velocity contour of un- shrouded (bare) rotor at first position.

The influence of shroud is also found in the space between the shroud wall and rotor, where the flow is accelerated. This phenomenon appear the main effects of shroud to rotor in focusing the stream and decreasing the slip flow.

5.2 Second Position: Rotor Blades in Parallel to the Free Stream

Here, the effect of the flange of the shroud is shown and obtained in the pressure contours at "figures 18, 19, 20 and 21". There are two highest pressure zones at the flanges of shroud, which were formatted due to the vortices. The flow velocity is increased based on the pressure difference between the inlet and outlet diffuser according to the momentum and continuity equations.

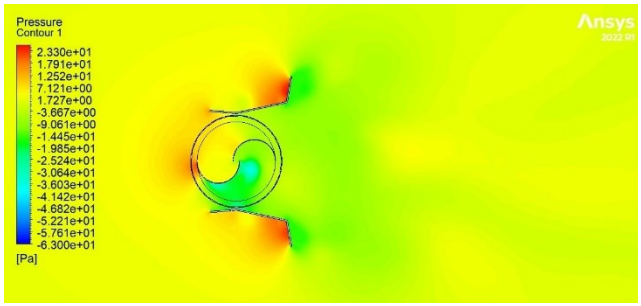


Fig. 18. Pressure contour of short flanged shrouded rotor at second position.

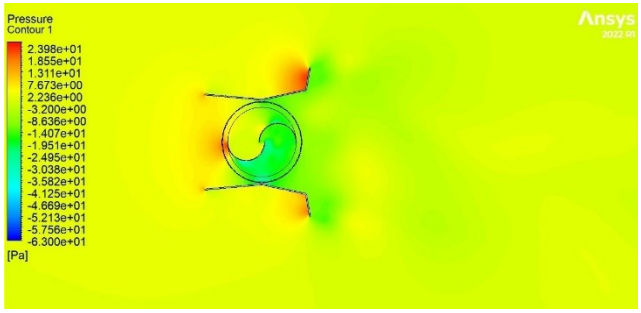


Fig. 19. Pressure contour of medium flanged shrouded rotor at second position.

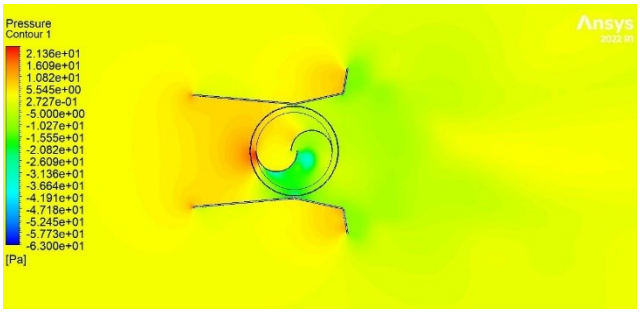


Fig. 20. Pressure contour of long flanged shrouded rotor at second position.

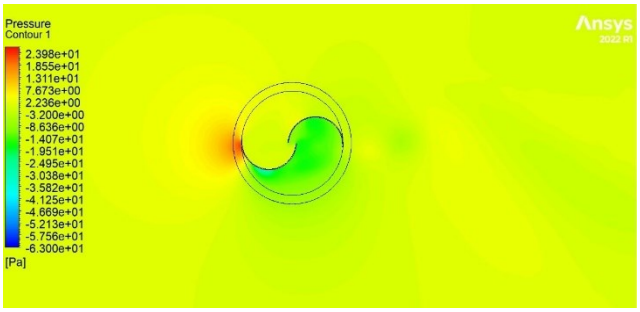


Fig. 21. Pressure contour of un-shrouded rotor at second position.

From previous figures, the pressure in the entrance was increasing in proportion to the entrance length of the shroud, whereas the un-shrouded rotor was not loaded with any pressure except for the facing area of the leading blade shown in "Figure 21".

It is concluded that the increase in velocity through the shroud was generated by the pressure difference between the pressure inlet, which is high, and the low pressure zone after the flange. The acceleration of the free stream is shown in figures 22, 23, 24, and 25, where the effect of the pressure difference on the velocities is very clear.

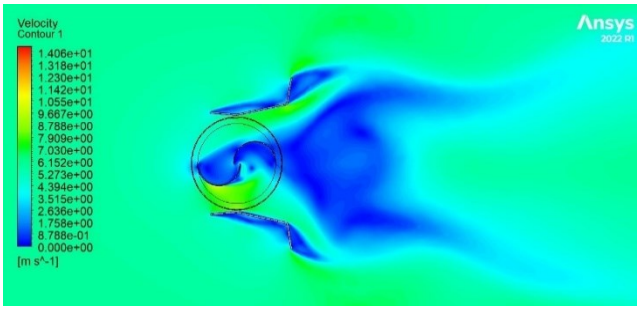


Figure 22. Velocity contour of short flanged shrouded rotor at second position.

The rotor torque values (T) against rotational speeds (ω) are extracted from ANSYS-FLUENT result files for three different models of shrouded rotors and un-shrouded rotors. The power and torque coefficients and tip speed ratio are calculated by Eqs. (3), (4), and (5) in all cases to get the curves of the torque and power coefficients against the tip speed ratio.

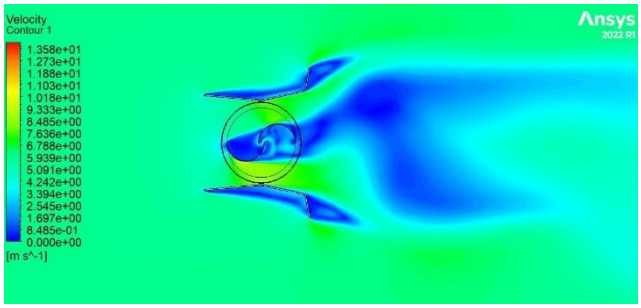


Fig. 23. Velocity contour of medium flanged shrouded rotor at second position.

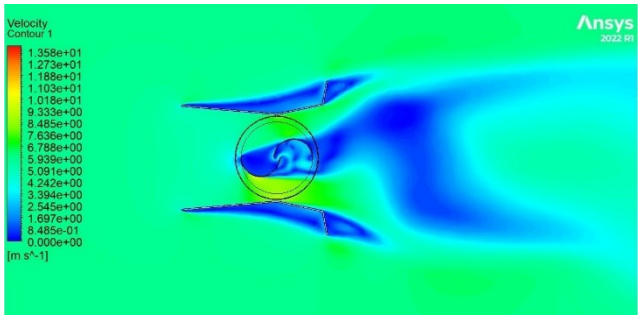


Fig. 24. Velocity contour of long flanged shrouded rotor at second position.

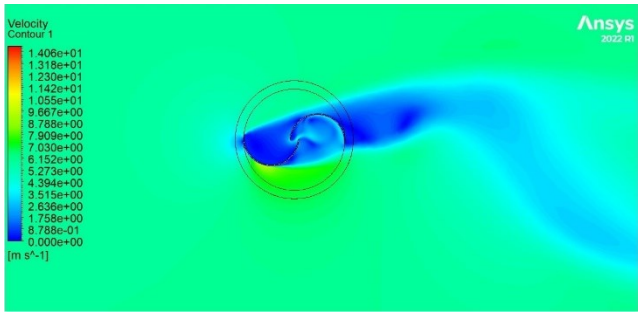


Fig. 25. Velocity contour of un-shrouded(bare)rotor at second position.

$$Ct = (4\ T)/ (\rho\ U2\ D2\ H) \quad (3)$$

$$Cp = (2\ T\ \omega)/ (\rho\ U3\ D\ H) \quad (4)$$

$$\lambda = (\omega.D) / (2.U) \quad (5)$$

In "Figure 26", it is shown that the medium- and long-shrouded Savonius rotor has the maximum torque coefficient of 0.35 at a tip speed ratio of 0.42. In "Figure 27", it is shown that the medium-shrouded Savonius rotor has the maximum C_p of 0.178 at λ 0.5, but it is not effective after a tip speed ratio of 0.7.

6. Conclusion

In this research, the effect of three different entrance lengths of flanged shroud Savonius rotors was 3-D numerically studied by ANSYS-FLUENT 2022 R1. The numerical model of this case is validated by comparing the current numerical power curve of the simulation model with

the previously published experimental power curve for the similar model at the same operation conditions, and it is found that the SST K-ω turbulence model at time step size 0.0025 s is the proper model for these cases.

The numerical results of this study indicate the following:

The shrouded rotor with different entrance lengths has the capability to capture more wind energy than the bare one.

The long and medium shroud rotor models have a maximum torque coefficient of 0.35 at a tip speed ratio of 0.42, which means a 27% increase in torque compared with the un-shrouded (bare) type.

The long-shrouded rotor has the maximum power coefficient of 0.178 at tip speed ratio 5, which means a 17% increase in power compared with the un-shrouded (bare) type.

The effect of using a plate obstacle at the entrance of the shroud on the performance of simple Savonius rotor can be considered as a future work. This will result in decreasing the negative drag force on the returning blade, which in turn, in addition to the flow acceleration by the shroud, might lead to a remarkable performance of the Savonius. Also, examining the effect of different shapes of Savonius rotor such as twisted rotor and developed rotor profile with the flanged shroud is planned for the future.

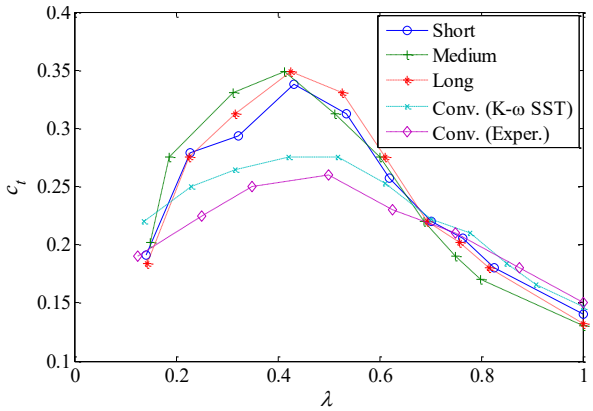


Fig. 26. Torque coefficient of shrouded and un-shrouded (bare) rotor against tip speed ratio.

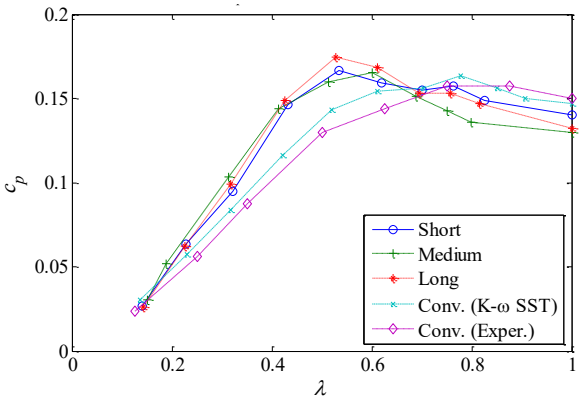


Fig. 27. Power coefficient of shrouded and un-shrouded (bare) rotor against tip speed ratio.

References

[1] F. Ayadi, I. Colak, I. Garip and H. I. Bulbul, "Targets of countries in renewable energy", 9th International Conference on Renewable Energy Research and Application (ICRERA), 2020.

[2] R. Atia and N. Yamada, "Distributed renewable generation and storage systems sizing in deregulated energy markets" International Conference on Renewable Energy Research and Applications (ICRERA), 2015.

[3] M. Cakir, I. Cankaya, I. Garip and I. Colak "Advantages of using renewable energy sources in smart grids", 10th International Conference on Smart Grid (icSmartGrid), 2022.

[4] Global Wind Energy Council (GWEC), 2023. Global Wind Report 2023, 20 August 2023.

[5] A. Amini and M. Kamoona "Hidden wind farms potential for residential households having roof-mounted wind arrester", International Conference on Renewable Energy Research and Application (ICRERA), 2014.

[6] A. T. Kaadan, M. Endo, M. Uruta and T. Yasuda, "Implementation of VAWT in energy generation decentralization in developing countries social, engineering & open data case study in South-East Asia", 7th International Conference on Renewable Energy Research and Applications ,(ICRERA), 2018.

[7] S. J. Savonius, "The S-rotor and its applications", Mech Eng., 53 (5), pp. 333-338, 1931.

[8] M. A. Abdelmordy, A. M. Abdelsalam, I. M. Sakr, and K. A. Ibrahim, "Numerical and experimental investigation of the ducted wind turbine performance with and without obstacle plates", ERJ, PART 2, Mech. Eng., Vol. 46, No. 1, pp. 21 - 31, January 2022.

[9] T. Ogawa and H. Yoshida, "The Effects of deflecting plate and rotor end plates on performances of savonius-type wind turbine", Bulletin of JSME, Vol. 29, No. 25, pp. 2115-2121, July 1986.

[10] B. D. Altan, M. Atilgan and A. Ozdamar, "An experimental study on improvement of a Savonius rotor performance with curtaining", Experimental Thermal and Fluid Science Vol. 32, No. 8, pp. 1673–1678, September 2008.

[11] K. M. Youssef, A. M. El-Kholy, A. M. Hamed, N. A. Mahmoud, A. M. El-Baz, and T. A. Mohamed, "An innovative augmentation technique of savonius wind turbine performance", Wind Engineering, Vol. 44, No. 1, pp. 1-20, May 2019.

[12] H. Zhang, Z. Li, D. Xin, and J. Zhan, "Improvement of aerodynamic performance of savonius wind rotor using straight-arc curtain", Applied sciences, Vol. 10, No. 20, pp. 7216, October 2020.

[13] T. Yuwono, G. Sakti, F.N. Aulia, and A.C. Wijaya, "Improving the performance of savonius wind turbine by installation of a circular cylinder upstream of returning turbine", Alexandria Engineering Journal, Vol. 59, No. 6, pp. 4923–49327, December 2020.

[14] M. H. Mohamed, F. Alqurashi, and D. Thevenin, "Performance enhancement of a savonius turbine under effect of frontal guiding plates", Energy Reports, Vol. 7, pp. 6069-6076, November 2021.

[15] M. H. Mohamed, G. Janiga, E. Pap, and D. Thevenin, "Optimal blade shape of a modified savonius turbine using an obstacle shielding the returning blade", Energy Conversion and Management, Vol. 52, No. 1, pp. 236–242, January 2011.

[16] S. Kaprawi, D. Santoso and R. Sipahutar, "Performance of Combined Water Turbine Darrieus-Savonius with Two Stage Savonius Buckets and Single Deflector", Internatıonal Journal of Renewable Energy Research, Vol. 5, No. 1, March 2015.

[17] M. R. Shouman, M. M. Helal, A. A. El-Haroun, "Numerical prediction of improvement of a Savonius rotor performance with curtaining and fin addition on blade", Alexandria Engineering Journal, Vol. 61, No. 12, pp. 10689–10699, December 2022.

[18] W. Tian, J. Bian, G. Yang, X. Ni, and Z. Mao, "Influence of a passive upstream deflector on the performance of the Savonius wind turbine", Energy Reports, Vol. 8, pp. 7488–7499, November 2022. (Article)

[19] W. Senarathna, M. Fernando, T. Silva., and C. Abeykoon, "The design of a savonius wind turbine with guide vanes - a computational approach", Proceedings of the 6th International Conference on Energy Harvesting, Storage, and Transfer (EHST22), Niagara Falls, Canada, Paper No. 133 DOI: 10.11159/ehst22.133, June 2022.

[20] Z. Mu, G. Tong, Z. Xiao, F. Feng, Y. Li, and G.V. Arne, "Study on aerodynamic characteristics of a savonius wind turbine with a modified blade", Energies, Vol. 15, No. 18, July 2022.

[21] P. Apparavoo1, S. Roy, and Y. San, "Performance study of savonius style wind turbines in a solar chimney power plant under guided flow environment", IOP Conf. Series: Earth and Environmental Science, Sci. 1074 012011, 2022.

[22] W. Yahya, K. Ziming, W. juan, and M. S. Qurashi, "Influence of tilt angle and the number of guide vane blades towards the Savonius rotor performance", Energy Reports, Vol. 7, pp. 3317-3327, November 2021.

[23] I. H. Siregar, M. Effendy, and A. H. A. Rasyid, "The effect of the number of vanes in the omnidirectional guide vane on aerodynamics characteristic of stationary swirling savonius rotor", International Journal of Mechanical Engineering and Robotics Research Vol. 10, No. 8, August 2021.

[24] A. H. Elbatran, Y. M. Ahmed and A. S. Shehata, "Performance study of ducted nozzle Savonius water turbine, comparison with conventional Savonius turbine", Energy, Vol. 134, pp. 566-584, September 2017.

[25] K. Irabu and J. N. Roy, "Characteristics of wind power on savonius rotor using a guide-box tunnel", Experimental Thermal and Fluid Science, Vol. 32, No. 2, pp. 580–586, November 2007.

[26] M. Mohammadi, R. Mohammadi, A. Ramadan, and M. H. Mohamed, "Numerical ınvestigation of performance refinement of a drag wind rotor using flow augmentation and momentum exchange optimization", Energy, Vol. 158, pp. 592-60, September 2018.

[27] E. Anter and M. Elkhoury, "Parametric sizing optimization process of a casing for a Savonius Vertical Axis Wind Turbine", Renewable Energy, Vol. 136, pp. 127-138, June 2019.

[28] N. Fuijisawa, "On the torque mechanism of Savonius rotors", Journal of Wind Engineering and Industrial Aerodynamics", Vol. 40, No. 3, pp. 277-292, 1992.

[29] N. Fuijisawa and F. Gotoh, "Visualization study of the flow in and around a savonius rotor", Experiments in Fluids", Vol. 12, pp. 407-412, April 1992.

[30] A. M. El-Zahaby, A. E. Kabeel, S. S. Elsayed and M. F. Obiaa, "CFD analysis of flow fields for shrouded wind turbine's diffuser model with different flange angles", Alexandria Engineering Journal, Vol. 56, No. 1, pp. 171-179, March 2017.